EURADOS intercomparison exercise on Monte Carlo modelling of a medical linear accelerator.

Barbara Caccia, Maïwenn Le Roy, Valentin Blideanu, Claudio Andenna, Chairmadurai Arun, Damian Czarnecki, Tarek El Bardouni, Régine Gschwind, Nicolas Huot, Eric Martin, et al.

EURADOS intercomparison exercise on monte carlo modelling of a medical linear accelerator

Barbara Caccia[1], Maïwenn Le Roy[2], Valentin Blideanu[2], Claudio Andenna[3], Chairmadurai Arun[4], Damian Czarnecki[5], Tarek El Bardouni[6], Régine Gschwind[7], Nicolas Huot[8], Eric Martin[7], Klemens Zink[5], Mariam Zoubair[6], Robert Price[9] and Loïc de Carlan[2]

[1]National Centre for Radiation Protection and Computational Physics, Istituto Superiore di Sanità and INFN, Roma, Italy
[2]CEA, LIST, Laboratoire National Henri Becquerel (LNE-LNHB), CEA-Saclay 91191 Gif-sur-Yvette Cedex, France
[3]INAIL-DIT, Roma, Italy
[4]Jaypee Hospital, Noida, India
[5]Institut fur Medizinische Physik und Strahlenschutz, Giessen, Germany
[6]Université Abdelmalek Essaadi, faculté des Sciences, Tétouan, Morocco
[7]IRMA/Chrono-Environnement – UMR CNRS 6249, Université de Franche-Comté, France
[8]CEA, DEN/DANS/DRSN/SEROS, 91191 Gif-sur-Yvette, France
[9]Inrad-Medical, Market Drayton, UK

Corresponding author:
Barbara Caccia
Centro Nazionale per la Protezione dalle Radiazioni e Fisica Computazionale
Istituto Superiore di Sanità
Viale Regina Elena, 299 00161 Roma
Tel. 06 49902889
e-mail: barbara.caccia@iss.it

Running title: EURADOS intercomparison: modelling of a linac

ABSTRACT

Background. In radiotherapy, Monte Carlo (MC) methods are considered a gold standard to calculate accurate dose distributions, particularly in heterogeneous tissues. EURADOS organized an international comparison with six participants applying different MC models to a real medical linear accelerator and to one homogeneous and four heterogeneous dosimetric phantoms.
Aims. The aim of this exercise was to identify, by comparison of different MC models with a complete experimental dataset, critical aspects useful for MC users to build and calibrate a simulation and perform a dosimetric analysis.
Results. Results show on average a good agreement between simulated and experimental data. However, some significant differences have been observed especially in presence of heterogeneities. Moreover, the results are critically dependent on the different choices of the initial electron source parameters.
Conclusions. This intercomparison allowed the participants to identify some critical issues in MC modelling of a medical linear accelerator. Therefore, the complete experimental dataset assembled for this intercomparison will be available to all the MC users, thus providing them an opportunity to build and calibrate a model for a real medical linear accelerator.

Keywords: Health Physics; Radiotherapy; Monte Carlo methods; Radiation Protection

INTRODUCTION

Monte Carlo (MC) radiation transport simulations have been used extensively for benchmarking photon dose calculations in modern radiotherapy [1]. The primary drawback of many commercial treatment planning systems (TPSs) is that they do not adequately model electron transport so that they produce significant errors (10% or more) near interfaces of low- or high-density inhomogeneity such as lung and bone [2, 3]. The magnitude of errors in the calculated dose distributions depends on photon energy, field size and the dose calculation point [4, 5, 6, 7]. It is well known that MC simulation of radiation transport is currently the most accurate means of predicting dose in complicated geometries [8] and an independent MC simulation can be used to validate commercial TPS. The major shortcoming of the MC method is that it is inherently a computationally intensive method. However, with the development of computer technology and variance reduction techniques, the MC method is becoming also a practical approach for accurate radiotherapy applications. Comparisons of MC simulations with benchmark experiments are important to evaluate the accuracy of MC calculated results. The European Radiation Dosimetry Group (EURADOS) has been organizing dosimetric intercomparisons for many years. In 2010 an intercomparison exercise was proposed by EURADOS with the aim of comparing the results obtained when different MC code users apply different MC models to simulate a well characterized medical linear accelerator (linac), with models differing by MC code and other parameters, such as the initial electron beam parameters and voxel size. In this work, methods and results of this intercomparison exercise for six different participants are reported. The exercise has been focused on relative dose distributions in both a homogeneous water phantom and different heterogeneous phantoms for a nominal 12-MV photon beam.

MATERIALS AND METHODS

Description of the exercise

The intercomparison exercise was carried out using the Laboratoire National Henri Becquerel (CEA, LIST, LNE-LNHB) accelerator facility, a Saturne 43 General Electric linear accelerator dedicated to establishing national references of absorbed dose to water for high-energy photon and electron beams. This accelerator provides 6 MV, 12 MV and 20 MV photon fields [9]. Participants were asked to model the 12 MV photon beam of the Saturne 43 linac for a 10x10 cm² field size defined at 100 cm from the source.

Task 1: modelling of the linac head.

All relevant geometry and material data were provided to the participants. In order to provide a realistic scenario, these data were typical of those usually available from linac manufacturers. Once the geometrical model of the linac head was generated, participants were asked to adjust the primary electron source parameters (energy distribution and electron spot size). To do so, participants were given experimental data measured at LNE-LNHB in a homogeneous 40x40x40 cm^3 water phantom at a distance of 90 cm from the source on the beam axis. Those were a depth dose curve measured on the beam axis with a plane-parallel NACP-02 ionization chamber (10 mm collecting electrode diameter) and a dose profile at 10 cm depth measured with a cylindrical PTW 31002 ionization chamber (0.125 cm^3).

The suggested procedure for adjusting the electron source parameters was the following: i) tuning of the energy: energy of the primary electrons is set according to the manufacturer specifications and then tuned until the calculated depth dose curve matches the measured one; ii) tuning of the electron spot size: with that energy, the electron spot size is changed until the calculated profile matches the measured one. For this task, participants were asked to provide the chosen electron source parameters, the spectral fluence distribution (calculated in air, 90 cm from the source on the beam axis), the calculated depth dose curve and dose profile as well as some relevant simulation parameters, such as photon and electron energy cutoff and voxel size. The ratio of the calculated absorbed dose at 10 cm to the number of primary electrons, used in task 2 for normalization, was also requested. Figure 1 shows a schematic view of the irradiation geometry.

Task 2: calculations with heterogeneities

The second task was dedicated to the calculations of relative absorbed dose distributions in four heterogeneous phantoms using the model designed in the first task. Diagrams of these phantoms are reported in figure 2. They are made of tissue equivalent slabs (lung and/or bone) immersed in the water phantom used in task 1. Participants were given all data related to geometry and materials. They were asked to provide dose distribution at points for which measurements with a PTW 31002 ionization chamber were available: depth dose curve upstream and downstream of the heterogeneity for phantoms A, B and C and dose profile at 22 cm and 25 cm depth for phantom D. These dose distributions were to be normalized using the ratio “absorbed dose at 10 cm/primary electron” calculated in task 1. Details about the heterogeneous phantoms and the corresponding measurements can be found in Blazy et al [10].

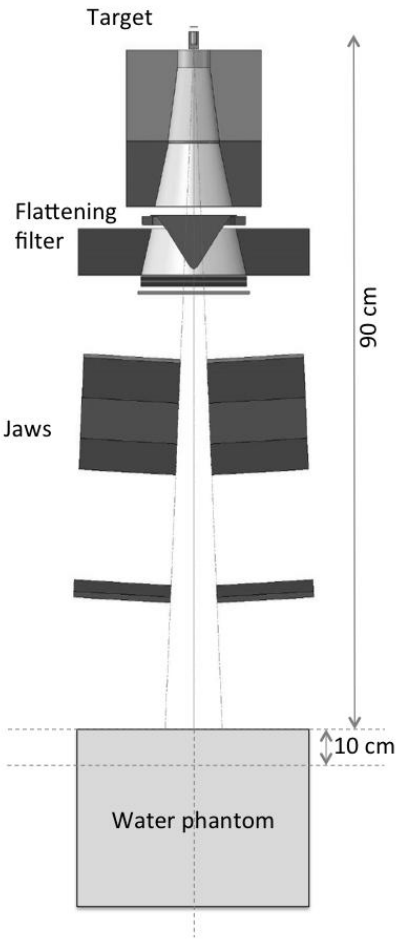

Figure 1. Schematic view of the simulated irradiation geometry for Saturne 43 General Electric linear accelerator. The 10x10 cm² field size is defined at 100 cm from the source, 10 cm below the phantom surface. The diagram is not to scale.

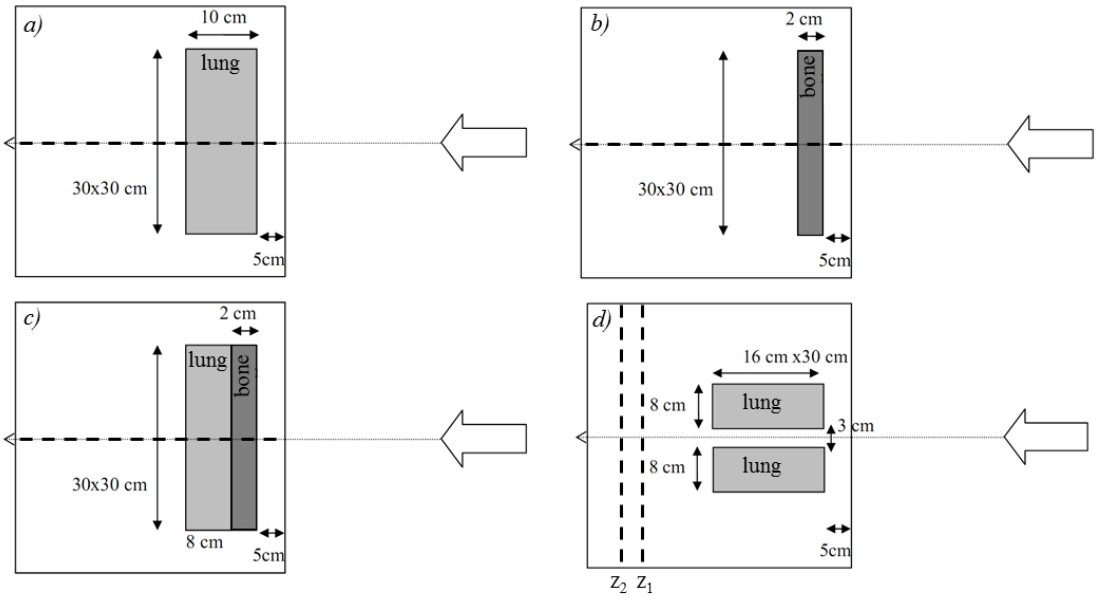

Figure 2. Diagrams of four heterogeneous phantoms. Each water phantom includes tissue equivalent heterogeneities: a) lung-equivalent tissue slab (phantom A); b) bone-equivalent tissue slab (phantom B); c) bone-

equivalent and lung-equivalent tissue slabs (phantom C); d) two lung-equivalent tissue slabs (phantom D). The diagrams are not to scale.

Evaluation of participants' results

As regards task 1, agreement between participants calculated and LNHB measured depth dose curves and dose profiles in the water phantom were evaluated using the gamma index [11, 12]. The distance to agreement criterion was set to 1 mm. The dose difference ΔD criterion was set to 1 %: it refers to a global gamma index i.e. ΔD is a percent dose relative to a global normalization point [13]. Here the normalization point is chosen to be the dose on the axis at 10 cm depth (which is also used for normalization of measurements and calculations for task 2). As pointed out by Depuydt et al. [14], when using a gamma index evaluation in a discrete environment, the sampling rate of the compared distributions (here calculations by participants) must be small with respect to the acceptance criteria. Thus, participants' results were sampled using linear or polynomial interpolation with a rate of 0.1 mm.

For task 2, gamma index 1%-1mm was calculated as stated above but k=2 uncertainties were also taken into account since, for some participants, the high statistical uncertainties on calculations could lead to a gamma index unjustly larger than one. Thus the passing rate when comparing measured and calculated dose distribution in the heterogeneous phantoms was defined as the percentage of points that satisfied $\gamma \leq 1$ or $|\Delta(\text{measurements-MC})| \leq U(\Delta(\text{measurements-MC}), k=2)$. Note that uncertainties were not taken into account for task 1 since passing the gamma index 1%-1mm was an objective given to participants when adjusting electron source parameters.

RESULTS AND DISCUSSION

There were six responses to the exercise, coming from five countries. Three results were obtained using different versions of BEAMnrc codes [15]: BEAMnrc-DOSXYZnrc version 4.2.3.1 and BEAMnrc version 4. The other three were obtained with GEANT4 (version 9.2) [16], MCNPX (version 2.5) [17] and TRIPOLI (version 4.7) [18].

Task 1: modelling of the linac head

Electron source parameters.

The parameter settings for the initial electron beam, as chosen by different participants, are shown in table 1. The first column indicates the identification code for each participant. The second column refers to the chosen electron energy distribution: the type of distribution and the characteristic parameters are indicated. The last column lists the characteristic of the electron beam spot. As reported in Verhaegen et al. [19] and Fix et al. [20] the definition of parameters for the electron beam spot is an important aspect of the MC simulation. In this case different parameter settings were chosen by the participants, even for those using the same MC code.

Table 1. Electron source parameters chosen by participants.

Participant ID	Electron energy distribution	Electron beam spot
#1	Gaussian - Mean: 12.3 MeV FWHM: 0.290 MeV	Circular homogenous Diameter: 2 mm
#2	Gaussian - Mean: 11.7 MeV FWHM: 1.17 MeV	Circular Gaussian FWHM: 0.5 mm 0.5° divergence
#3	Monoenergetic 11.25 MeV	Point-like
#4	Gaussian - Mean: 12 MeV FWHM: N/A	Circular homogeneous Diameter: 0.8 mm
#5	Gaussian - Mean: 11.4 MeV FWHM: 0.5 MeV	Circular Gaussian FWHM: 1.7 mm
#6	Monoenergetic 11.5 MeV	Circular homogeneous Diameter: 1.5 mm

Spectral fluence and absorbed dose per primary electron.
The reference values used for the normalization (i.e. the simulated absorbed dose in water at 10-cm depth per primary electron) and the mean energy calculated from photon spectral fluence are reported in table 2 for each participant. As regards the absorbed dose at 10 cm depth per primary electron, the value for the participant #4 is about 100-times higher than the mean value obtained by others participants, whereas for the participant #3 the value is twice the mean value obtained by the participant #1, #2, #5 and #6. These discrepancies could not be explained using the limited data provided by the participants but this illustrates that using Monte Carlo methods for absolute dose calculation are complex.
As regards the mean energy from photon spectral fluence, most values are within 3.50±0.05 MeV, with a higher value for participant #4. In figure 3 the relative photon spectral fluence is reported as a function of the energy, with thicker sections of the curve indicating a larger spread of values among participants.

Table 2. Reference value used for normalization and mean energy calculated from photon spectral fluence.

Participant ID	Absorbed dose in water at 10 cm depth per primary electron (Gy/electron)	Mean energy from spectral fluence (MeV)
#1	3.433E-16	3.52
#2	3.440E-16	3.54
#3	6.690E-16	3.47
#4	3.757E-14	3.64
#5	3.096E-16	3.46
#6	3.495E-16	3.43

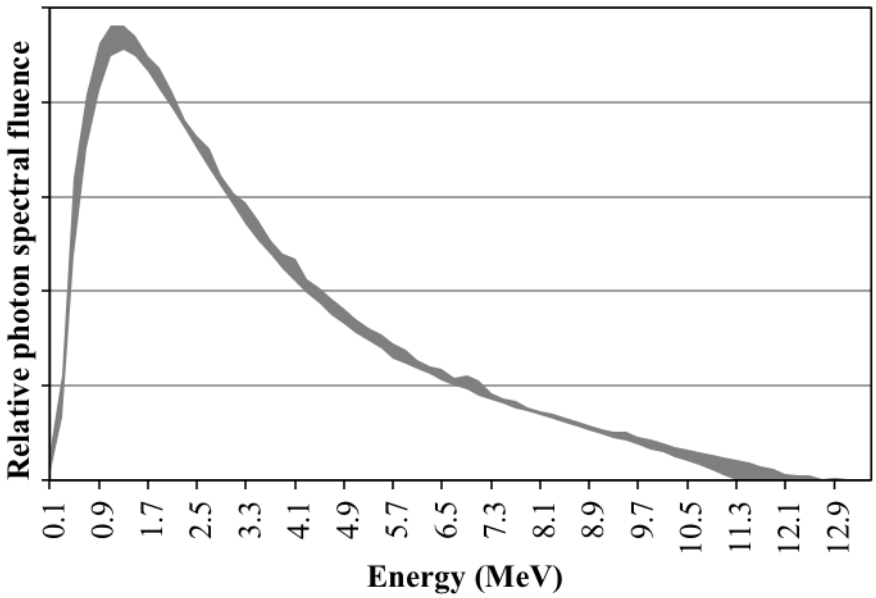

Figure 3. Range between minimal and maximal value obtained by all participants for spectral photon fluence.

Depth dose curves and dose profiles in the water phantom.
Relative statistical uncertainties associated with depth dose curve and dose profiles calculated in water are reported in table 3 (columns 2 and 3). They show differences depending on the voxel sizes and on the number of histories considered for the simulation by the different participants. The relative uncertainty associated to measurements is 0.7% (k=2).

Table 3. Relative statistical uncertainty associated to submitted results.

Participant ID	Statistical uncertainty (%) given by participants (*k*=2)			
	Depth dose curve in water[a]	Dose profile at 10 cm in water[b]	Depth dose curve in phantoms A,B,C (lung, bone, bone and lung)[c]	Dose profile at 22 and 25 cm in phantom D[b,d]
#1	0.06 to 0.10	0.07 to 0.5	0.04 to 0.1	0.08 to 0.3
#2	0.3	1.1 to 5.3	0.4 to 0.6	0.4 to 1.9
#3	0.7 to 1.1	0.8 to 4.9	1.0 to 1.7	1.8 to 7.7
#4	0.8 to 1.1	0.9 to 5.4	1.4 to 2.3	1.5 to 3.1
#5	0.5 to 2.3	0.5 to 2.3	0.4 to 2.1	0.8 to 3.2
#6	0.4 to 0.8	1.0 to 5.8	0.7 to 0.9	1.0 to 3.5

[a] Uncertainty increases at greater depth and in the build-up region
[b] Uncertainty increases when moving away from central axis
[c] Uncertainties were similar for these three cases for all participant
[d] Uncertainties similar at 22 or 25cm depth

The 1%-1mm gamma index values for depth dose curve and dose profiles are summarized in table 4 (columns 2 and 3). In figure 4 the depth-dose and the dose-profile curves are reported for the three participants (#1, #3 and #4) with a non-perfect passing rate of gamma index values. As for depth dose curves, all disagreements between measurements and calculations occur in the build-up area. This is not a surprise since in this region, accurate ion chamber measurements are difficult to make and calculations are very sensitive to the energy of the electron source [21, 22]. As regards dose profiles, disagreements occur mostly in the penumbra region and in the lateral "horn" area of the profile. This could be explained by the influence of both the mean energy of primary electrons and the electron spot size [21].

Table 4. 1%-1mm gamma index passing rate when comparing participant calculated dose distribution and LNHB measurements for depth dose curve and dose profile in water and heterogeneous phantoms

Participant ID	Passing rate 1%-1mm global gamma index		Passing rate (combination of 1%-1mm global gamma index and *k*=2 uncertainties)			
	Depth dose curve in water	Dose profile in water	Phantom A	Phantom B	Phantom C	Phantom D*
#1	87 %	91 %	56 %	78 %	72 %	95 %, 99 %
#2	100 %	100 %	86 %	95 %	100 %	99 %, 78 %
#3	94 %	78 %	86 %	75 %	89 %	52 %, 66 %
#4	98 %	91 %	92 %	90 %	83 %	78 %, 70%
#5	100 %	100 %	61 %	58 %	75 %	72 %, 67 %
#6	100 %	100 %	100 %	100 %	88 %	95 %, 94 %

* Data are referred to profiles in the phantom at depth of 22 cm (left values) and 25 cm (right values)

Task 2: calculations with heterogeneities

An overview of the results regarding the calculations with heterogeneities is shown in table 4 using the evaluation method presented in section 2.2. k=2 relative uncertainties on the calculations are found in Table 3. The relative uncertainty associated to measurements is 0.7% (k=2). Two questions can be asked looking at those results: 1) if the modelling of the linac and choice of electron source are correct in task 1, are the calculations in the presence of heterogeneities necessarily accurate? 2) as regards imprecise models designed in task 1, is there a propagation of the disagreements seen in the water phantom to the heterogeneous phantoms or what is the importance of the linac modelling and choice of electron source parameters?

Does a correct model lead to accurate calculations in presence of heterogeneities?
For participants #2 and #6 that had a 100% passing rate in the water phantom for depth dose curve and dose profile, it seems that a good model implies accurate calculations in presence of heterogeneities (passing rate superior to 85 % except for participant #2-phantom B).
However, this is not the case for participant #5 for whom, in spite of a perfect agreement with measurements in the water phantom, the passing rate in the presence of heterogeneities lies between 58 and 75 %. These low pass rates are due to an overestimation of dose before and after heterogeneities (figure 5). The most probable explanation for such overestimation is due to the use of the same thickness of phantom entrance window as in task 1. In fact, during the final internal review of this paper, participant #5 discovered to have not used for Task 2 the correct geometrical parameter for the phantom. Participant #5 repeated, with the correct geometrical parameter, one of the Task-2 simulations obtaining a better agreement with measurements.

Importance of the linac modelling and electron source parameters choice.
It seems quite evident that inaccurate modelling of the linac head or inadequate choice of electron source parameters can lead to disagreements between measurements and calculations in the presence of heterogeneities.
Firstly, electron source parameters chosen by participants are crucial for simulation of their effects in the build-up zones. This is well illustrated by the example of participant #1 for which underestimation of the dose in the build-up area in task 1 is present for phantoms A, B and C (see for example figure 6 for phantom A). It is worth mentioning that regardless of the participant, all disagreements between measurements and calculations for phantom A, B and C are located in the build-up zones.
The importance of electron source parameters can also be seen in the case of participant #3 for phantom D (two lung phantom). Indeed the disagreement between measurements and calculations encountered for the penumbra and horn areas of the dose profile in the water phantom can be found in the dose profiles calculated downstream of the lung heterogeneity (figure 7).

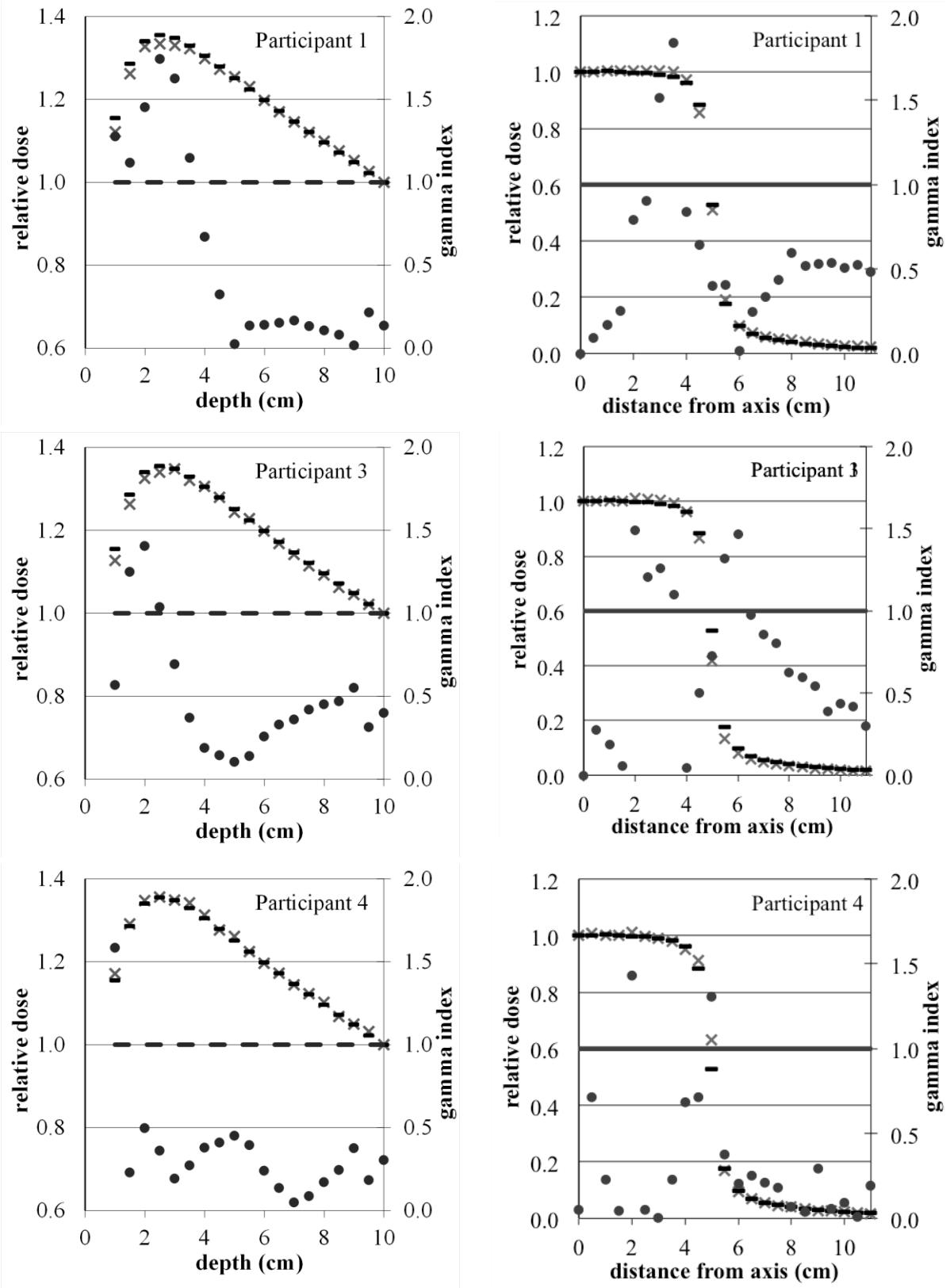

Figure 4. Depth dose curves and dose profiles (participants calculations (X) and measurements (-) data) and corresponding gamma index (**.**) (1%/1mm) for participants with non-perfect gamma index passing rate.

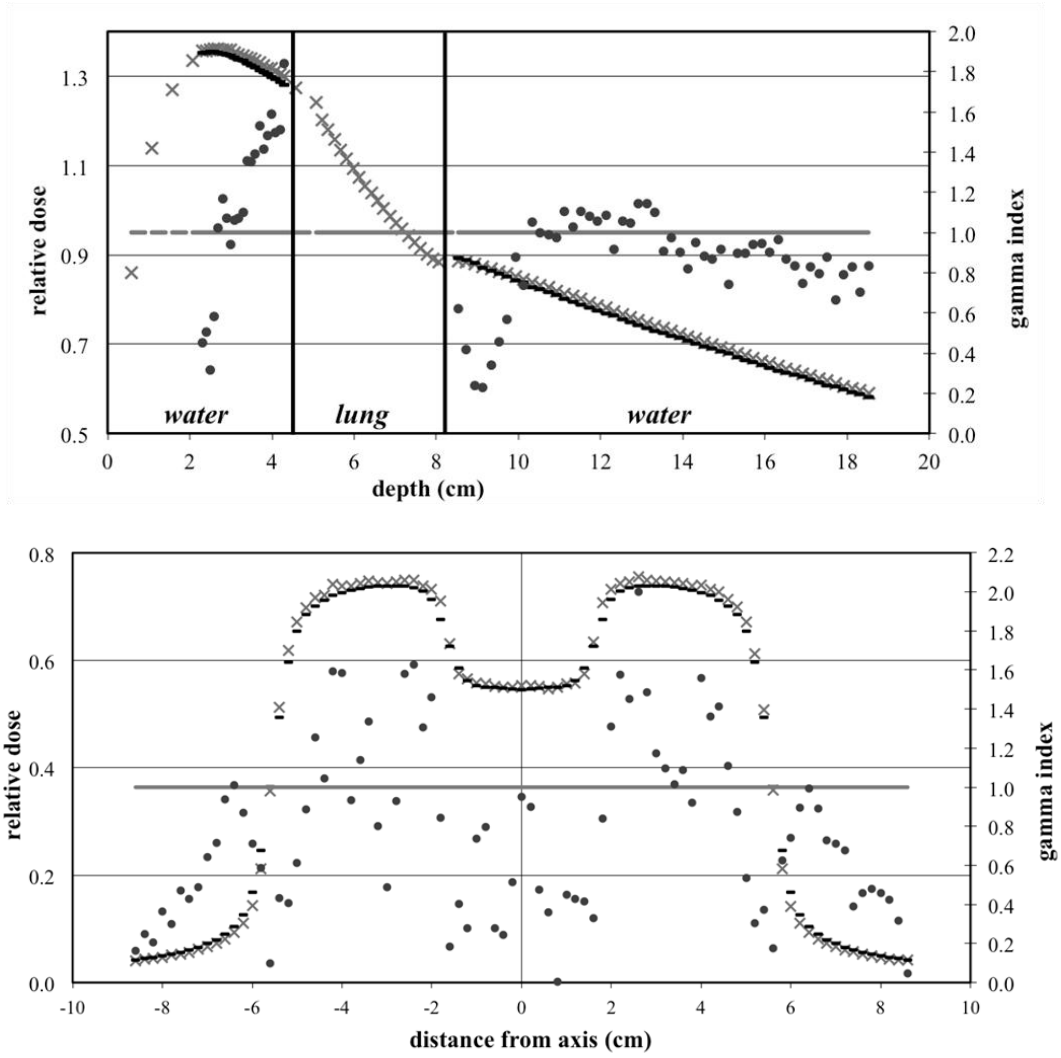

Figure 5. Depth dose curve and dose profile (participants calculations (X) and measurements (-) data) and corresponding gamma index (●) (1%/1mm) for participant #5 (phantom A and phantom D at 22 cm depth).

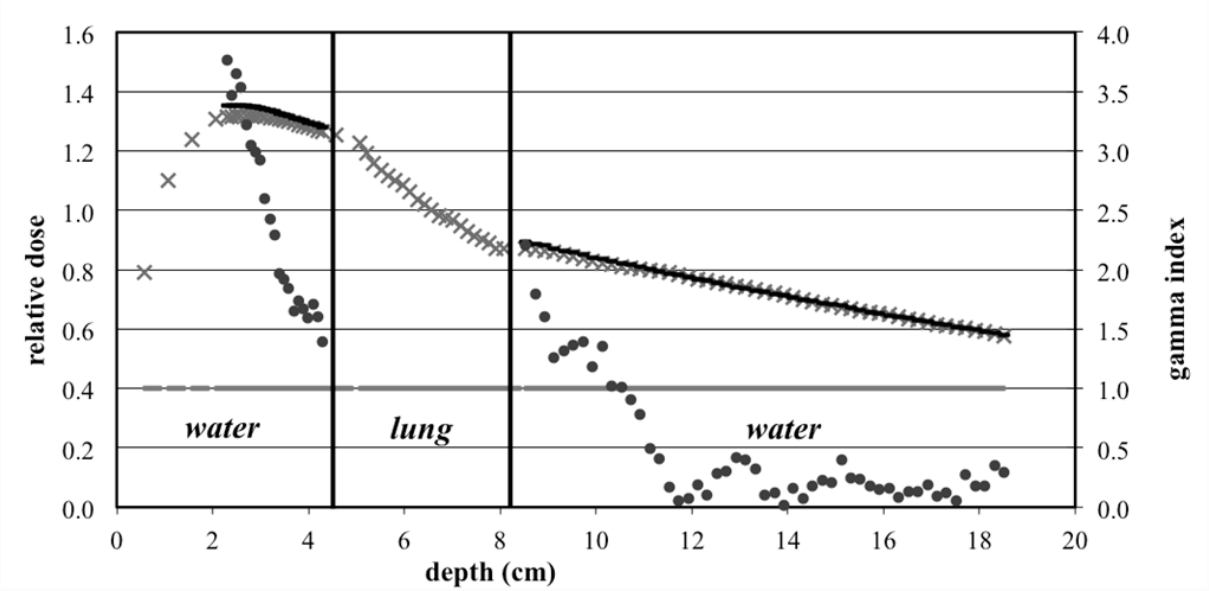

Figure 6. Depth dose curve (participants calculations (X) and measurements (-) data) and corresponding gamma index (.) (1%/1mm) for participant #1 (phantom A).

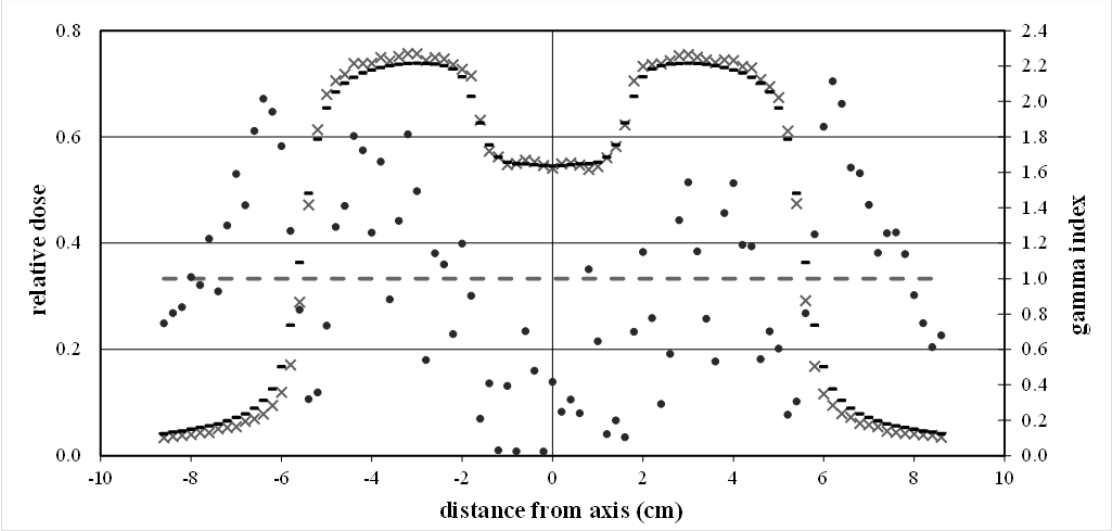

Figure 7. Dose profile (participants calculations (X) and measurements (-) data) and corresponding gamma index (.) (1%/1mm) for participant #3 (phantom D – 22 cm depth).

CONCLUSIONS

The results of this intercomparison exercise clearly show that there are different approaches for the determination of the initial electron beam characteristics, i.e. different geometrical model of the beam and different description of the electron source energy (even when using the same Monte Carlo code). Moreover, the results of dose distribution calculations in the presence of heterogeneities confirm the importance of electron source parameter choices: an inadequate model established using measurements in a water phantom inevitably leads to disagreements between calculations and measurements when adding heterogeneities. For example, discrepancies observed in the build-up area of the depth dose curve in the water phantom can lead to discrepancies at the boundaries between water and lung. On the other hand, a correct modelling of the linac head and electron source does not assure accurate calculations in presence of heterogeneities. The aim of this exercise was to help MC users to develop the skills needed to build and calibrate a MC simulation and perform a dosimetric analysis for a clinical linear accelerator, and to understand how well such calculations are likely to be performed in practice. Moreover, the opportunity to have a real dosimetric data set, including dosimetric data for different water phantoms with heterogeneities (bone and lung), and a full description of a linear accelerator, represents an opportunity for all the MC users to validate their code and their implementation of that code. All the data necessary to realize this exercise can be requested directly from the corresponding author.

ACKNOWLEDGEMENTS

This work was performed as part of the work programme of EURADOS Working Group 6, Computational Dosimetry, initially under the chairmanship of Dr Gianfranco Gualdrini (ENEA, Bologna, Italy - now retired) and subsequently under the chairmanship of Dr Rick Tanner (Public Health England, Chilton, UK).

REFERENCES

1. Rogers DWO. Fifty years of Monte Carlo simulations for medical physics. *Phys Med Biol* 2006;51:R287-R301. DOI:10.1088/0031-9155/51/13/R17.
2. Carrasco P, Jornet N, Duch MA, Weber L, Ginjaume M, Eudaldo T, Jurado D, Ruiz A and Ribas M. Comparison of dose calculation algorithms in phantoms with lung equivalent heterogeneities under conditions of lateral electronic disequilibrium. *Med Phys* 2004;31:2899-911. DOI: 10.1118/1.1788932.
3. Carrasco P, Jornet N, Duch M A, Panettieri V, Weber L, Eudaldo T, Ginjaume M, Ribas M. Comparison of dose calculation algorithms in slab phantoms with cortical bone equivalent heterogeneities. *Med Phys* 2007;34:3323-33. DOI: 10.1118/1.2750972.
4. Björk P, Knöös T and Nilsson P. Influence of initial electron beam characteristics on Monte Carlo calculated absorbed dose distributions for linear accelerator electron beams. *Phys Med Biol* 2002;47:4019-41. DOI:10.1088/0031-9155/47/22/308.
5. Das IJ, Cheng CW, Watts RJ, Ahnesjö A, Gibbons J, Li XA, Lowestein J, Mitra RK, Simon WE and Zhu C. Accelerator beam data commissioning equipment and procedures: report of the TG-106 of the Therapy Physics Committee of the AAPM. *Med Phys* 2008;35:4186-215. DOI: 10.1118/1.2969070.
6. Sterpin E, Chen Y, Lu W, Mackie TR, Olivera GH and Vynckier S. On the relationships between electron spot size, focal spot size, and virtual source position in Monte Carlo simulations. *Med Phys* 2011;38:1579-86. DOI: 10.1118/1.3556560.
7. Tzedakis A Damilakis JE Mazonakis M, Stratakis J, Varveris H and Gourtsoyiannis N. Influence of initial electron beam parameters on Monte Carlo calculated absorbed dose distributions for radiotherapy photon beams. *Med Phys* 2004;31:907-13. DOI: 10.1118/1.1668551.
8. Seco J and Verhaegen F. Monte Carlo techniques in radiation therapy. CRC press. Series: Imaging in Medical Diagnosis and Therapy. ISBN 9781466507920; 2013.
9. Mazurier J, Salvat F, Chauvenet B, Barthe J. Simulation of photon beams from a Saturne 43 accelerator using the code PENELOPE. *Phys Med* 1999;15:101-110.
10. Blazy L, Baltes D, Bordy JM, Cutarella D, Delaunay F, Gouriou J, Leroy E, Ostrowsky A and Beaumont S. Comparison of PENELOPE Monte Carlo dose calculations with Fricke dosimeter and ionization chamber measurements in heterogeneous phantoms (18 MeV electron and 12 MV photon beams). *Phys Med Biol* 2006;51:5951-65. DOI: 10.1088/0031-9155/51/22/016.
11. Low DA, Harms WB, Mutic S and Purdy JA. A technique for the quantitative evaluation of dose distributions. *Med Phys* 1998;25:656-61. DOI: 10.1118/1.598248.
12. Graves YJ, Jia X and Jiang SB. Effect of statistical fluctuation in Monte Carlo based photon beam dose calculation on gamma index evaluation. *Phys Med Biol* 2013;58:1839-53. DOI:10.1118/1.4814600.
13. Stojadinovic S, Ouyang L, Gu X, Pompoš A, Bao Q and Solberg TD. Breaking bad IMRT QA practice. *J Appl Clin Med Phys* 2015;16(3):154-65. DOI: 10.1120/jacmp.v16i3.5242.
14. Depuydt T, Van Esch A and Huyskens DP. A quantitative evaluation of IMRT dose distributions: refinement and clinical assessment of the gamma evaluation. *Radiother Oncol* **2002;**62:309-19. DOI: 10.1016/S0167-8140(01)00497-2.
15. Kawrakow I. Accurate condensed history Monte Carlo simulation of electron transport. I. EGSnrc, the new EGS4 version. *Med Phys* 2000;27:485-98. DOI:10.1118/1.598917.
16. Agostinelli S, Allison J, Amako KA, Apostolakis J, Araujo H, Arce P, Asai M, Axen D, Banerjee S and Barrand, G. GEANT4 - a simulation toolkit. *Nucl Instrum Methods Phys Res A* **2003;**506:250-303. DOI:10.1016/S0168-9002(03)01368-8.
17. Pelowitz DBE. MCNP6TM User's Manual Version 1.0. LA-CP-13-00634; 2013.
18. Brun E, Dumonteil E, Hugot FX, Huot N, Lee YK, Malvagi F, Mazzolo A, Petit O, Trama JC, Zoia A. Overview of TRIPOLI-4 version 7, Continuous-energy Monte Carlo Transport Code. In: *International Congress on Advances in Nuclear Power Plants 2011. Proceedings*. Nice: May 2-6, 2011. p. 1584-1589. ISBN: 978-1-61839-809-3.
19. Verhaegen F and Seuntjens J. Monte Carlo modelling of external radiotherapy photon beams. *Phys Med Biol* 2003;48:R107-64. DOI: 10.1088/0031-9155/48/21/R01.
20. Fix MK, Keall PJ and Siebers JV. Photon-beam subsource sensitivity to the initial electron-beam parameters. *Med Phys* 2005;32:1164-75. DOI: 10.1118/1.1884385.
21. Keall PJ, Siebers JV, Libby B and Mohan R. Determining the incident electron fluence for Monte Carlo-based photon treatment planning using a standard measured data set. *Med Phys* 2003;30:574-82. DOI: 10.1118/1.1561623.
22. Blazy L. Contrôle qualité des systèmes de planification dosimétriques des traitements en radiothérapie externe au moyen du code Monte-Carlo PENELOPE. Thesis Toulouse III University; 2003. http://thesesups.ups-tlse.fr/11/1/Blazy-Aubignac.pdf.

Figure captions

Figure 1. Schematic view of the simulated irradiation geometry. The 10x10 cm² field size is defined at 100 cm from the source, 10 cm below the phantom surface. The diagram is not to scale.

Figure 2. Diagrams of four heterogeneous phantoms. Each water phantom includes tissue equivalent heterogeneities: a) lung-equivalent tissue slab (phantom A); b) bone-equivalent tissue slab (phantom B); c) bone-equivalent and lung-equivalent tissue slabs (phantom C); d) two lung-equivalent tissue slabs (phantom D). The diagrams are not to scale.

Figure 3. Range between minimal and maximal value obtained by all participants for spectral photon fluence.

Figure 4. Depth dose curves and dose profiles (participants calculations (X) and measurements (-) data) and corresponding gamma index (•) (1%/1mm) for participants with non-perfect gamma index passing rate.

Figure 5. Depth dose curve and dose profile (participants calculations (X) and measurements (-) data) and corresponding gamma index (•) (1%/1mm) for participant #5 (phantom A and phantom D at 22 cm depth).

Figure 6. Depth dose curve (participants calculations (X) and measurements (-) data) and corresponding gamma index (•) (1%/1mm) for participant #1 (phantom A).

Figure 7. Dose profile (participants calculations (X) and measurements (-) data) and corresponding gamma index (•) (1%/1mm) for participant #3 (phantom D – 22 cm depth).

Table captions

Table 1. Electron source parameters chosen by participants.

Table 2. Reference value used for normalization and mean energy calculated from photon spectral fluence.

Table 3. Relative statistical uncertainty associated to submitted results.

Table 4. 1%-1mm gamma index passing rate when comparing participant calculated dose distribution and LNHB measurements for depth dose curve and dose profile in water and heterogeneous phantoms

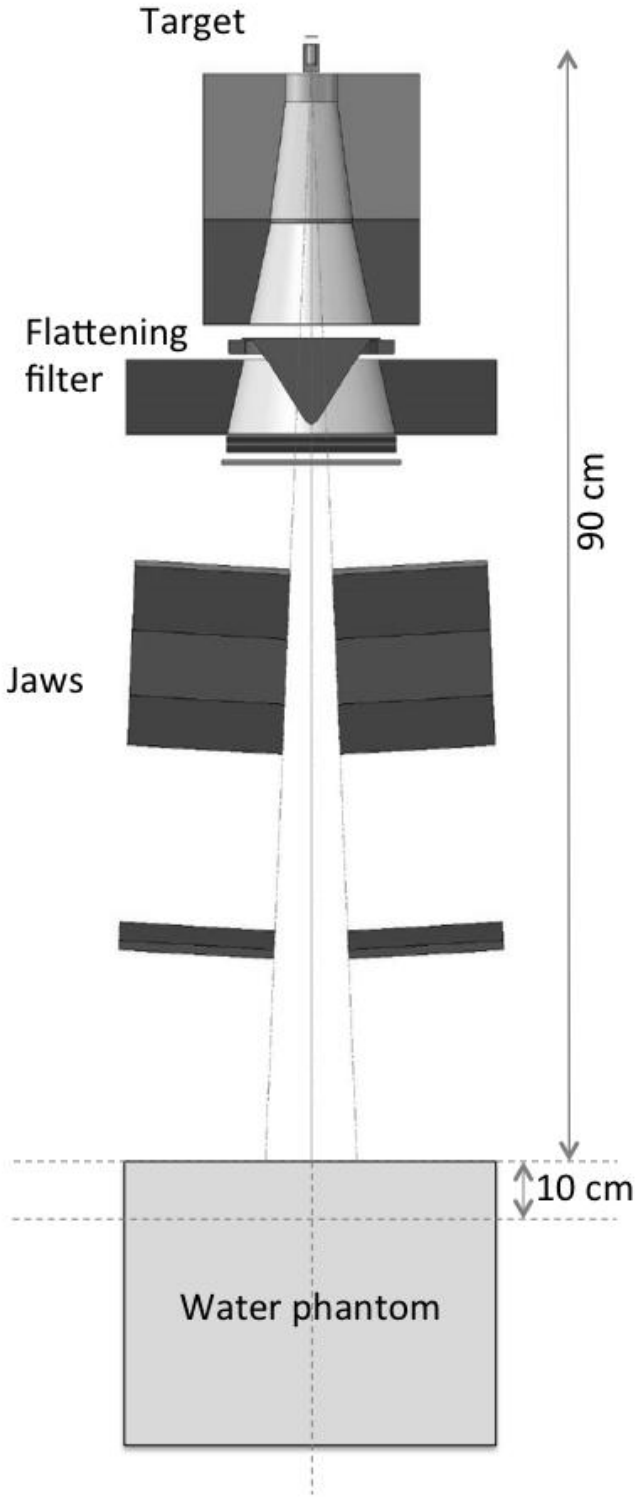

Figure 1. Schematic view of the simulated irradiation geometry for Saturne 43 General Electric linear accelerator. The 10x10 cm² field size is defined at 100 cm from the source, 10 cm below the phantom surface. The diagram is not to scale.

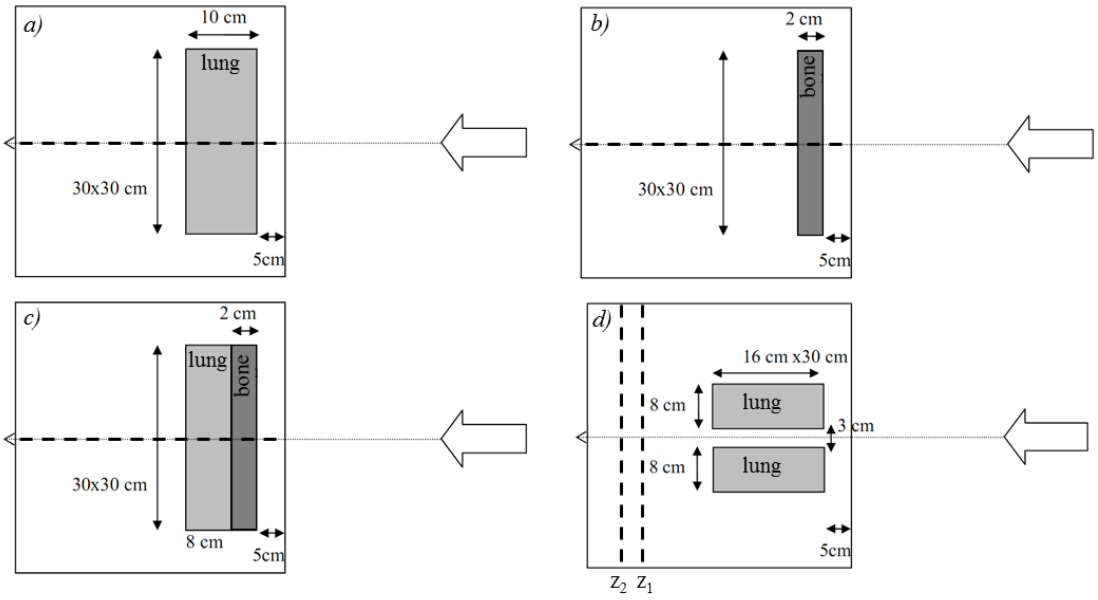

Figure 2. Diagrams of four heterogeneous phantoms. Each water phantom includes tissue equivalent heterogeneities: a) lung-equivalent tissue slab (phantom A); b) bone-equivalent tissue slab (phantom B); c) bone-equivalent and lung-equivalent tissue slabs (phantom C); d) two lung-equivalent tissue slabs (phantom D).). The diagrams are not to scale.

Table 1. Electron source parameters chosen by participants.

Participant ID	Electron energy distribution	Electron beam spot
#1	Gaussian - Mean: 12.3 MeV FWHM: 0.290 MeV	Circular homogenous Diameter: 2 mm
#2	Gaussian - Mean: 11.7 MeV FWHM: 1.17 MeV	Circular Gaussian FWHM: 0.5 mm 0.5° divergence
#3	Monoenergetic 11.25 MeV	Point-like
#4	Gaussian - Mean: 12 MeV FWHM: N/A	Circular homogeneous Diameter: 0.8 mm
#5	Gaussian - Mean: 11.4 MeV FWHM: 0.5 MeV	Circular Gaussian FWHM: 1.7 mm
#6	Monoenergetic 11.5 MeV	Circular homogeneous Diameter: 1.5 mm

Table 2. Reference value used for normalization and mean energy calculated from photon spectral fluence.

Participant ID	Absorbed dose in water at 10 cm depth per primary electron (Gy/electron)	Mean energy from spectral fluence (MeV)
#1	3.433E-16	3.52
#2	3.440E-16	3.54
#3	6.690E-16	3.47
#4	3.757E-14	3.64
#5	3.096E-16	3.46
#6	3.495E-16	3.43

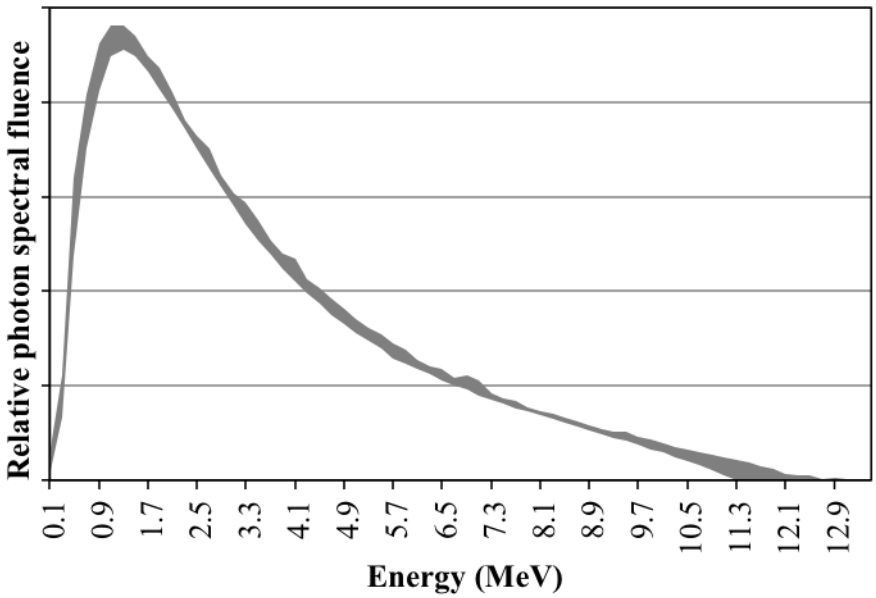

Figure 3. Range between minimal and maximal value obtained by all participants for spectral photon fluence.

Table 3. Relative statistical uncertainty associated to submitted results.

Participant ID	Statistical uncertainty (%) given by participants (k=2)			
	Depth dose curve in water[a]	Dose profile at 10 cm in water[b]	Depth dose curve in phantoms A,B,C (lung, bone, bone and lung)[c]	Dose profile at 22 and 25 cm in phantom D[b,d]
#1	0.06 to 0.10	0.07 to 0.5	0.04 to 0.1	0.08 to 0.3
#2	0.3	1.1 to 5.3	0.4 to 0.6	0.4 to 1.9
#3	0.7 to 1.1	0.8 to 4.9	1.0 to 1.7	1.8 to 7.7
#4	0.8 to 1.1	0.9 to 5.4	1.4 to 2.3	1.5 to 3.1
#5	0.5 to 2.3	0.5 to 2.3	0.4 to 2.1	0.8 to 3.2
#6	0.4 to 0.8	1.0 to 5.8	0.7 to 0.9	1.0 to 3.5

[a] Uncertainty increases at greater depth and in the build-up region
[b] Uncertainty increases when moving away from central axis
[c] Uncertainties were similar for these three cases for all participant
[d] Uncertainties similar at 22 or 25cm depth

Table 4. 1%-1mm gamma index passing rate when comparing participant calculated dose distribution and LNHB measurements for depth dose curve and dose profile in water and heterogeneous phantoms

Participant ID	Passing rate 1%-1mm global gamma index		Passing rate (combination of 1%-1mm global gamma index and *k*=2 uncertainties)			
	Depth dose curve in water	Dose profile in water	Phantom A	Phantom B	Phantom C	Phantom D*
#1	87 %	91 %	56 %	78 %	72 %	95 %, 99 %
#2	100 %	100 %	86 %	95 %	100 %	99 %, 78 %
#3	94 %	78 %	86 %	75 %	89 %	52 %, 66 %
#4	98 %	91 %	92 %	90 %	83 %	78 %, 70%
#5	100 %	100 %	61 %	58 %	75 %	72 %, 67 %
#6	100 %	100 %	100 %	100 %	88 %	95 %, 94 %

* Data are referred to profiles in the phantom at depth of 22 cm (left values) and 25 cm (right values)

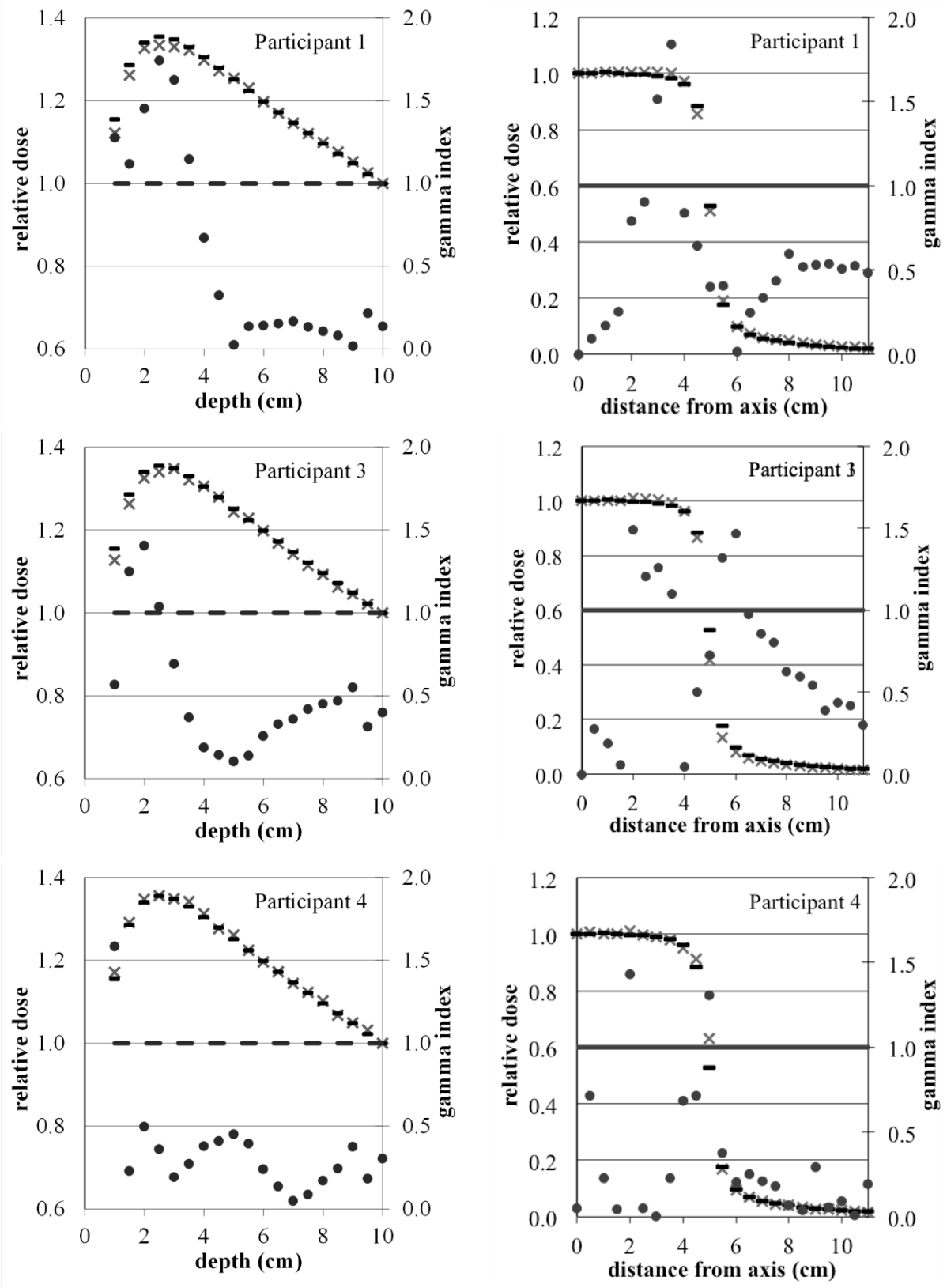

Figure 4. Depth dose curves and dose profiles (participants calculations (X) and measurements (-) data) and corresponding gamma index (.) (1%/1mm) for participants with non-perfect gamma index passing rate.

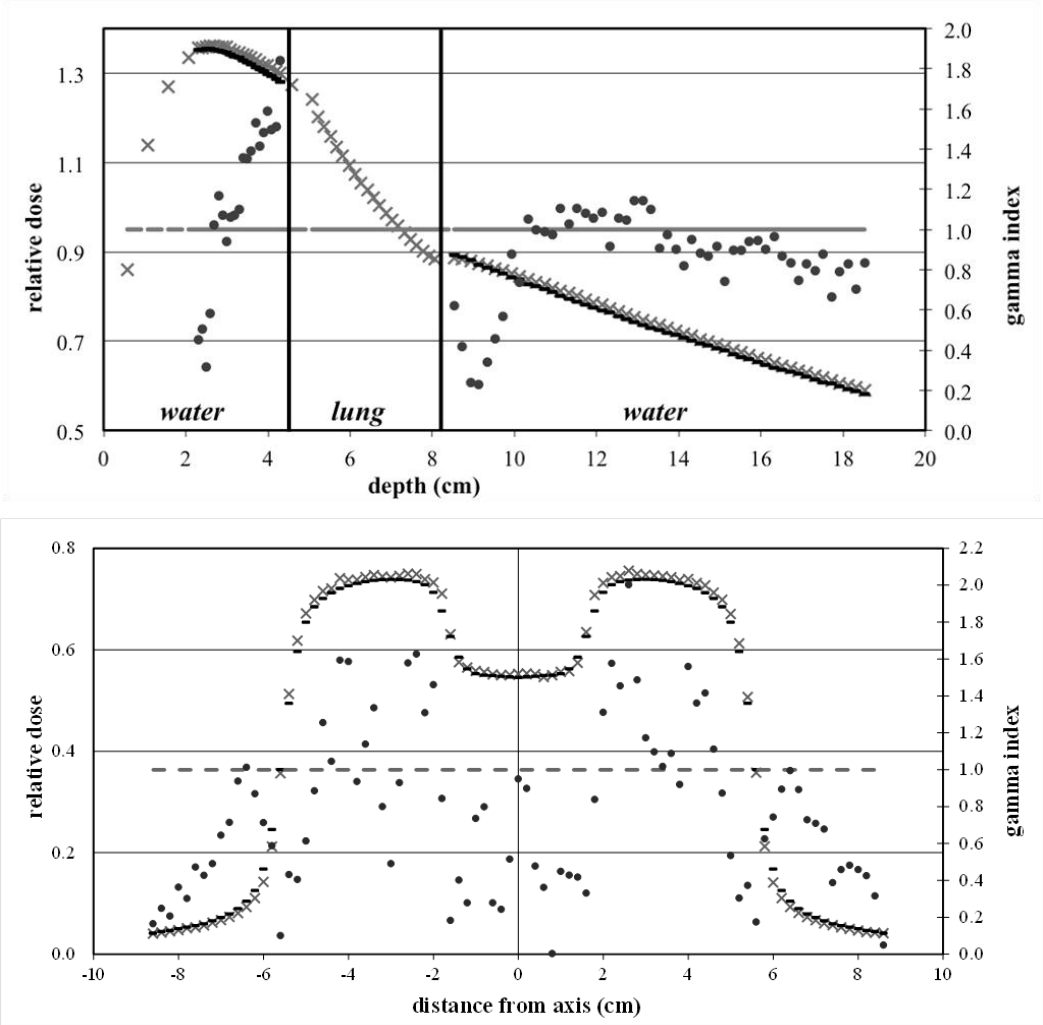

Figure 5. Depth dose curve and dose profile (participants calculations (X) and measurements (-) data) and corresponding gamma index (●) (1%/1mm) for participant #5 (phantom A and phantom D at 22 cm depth).

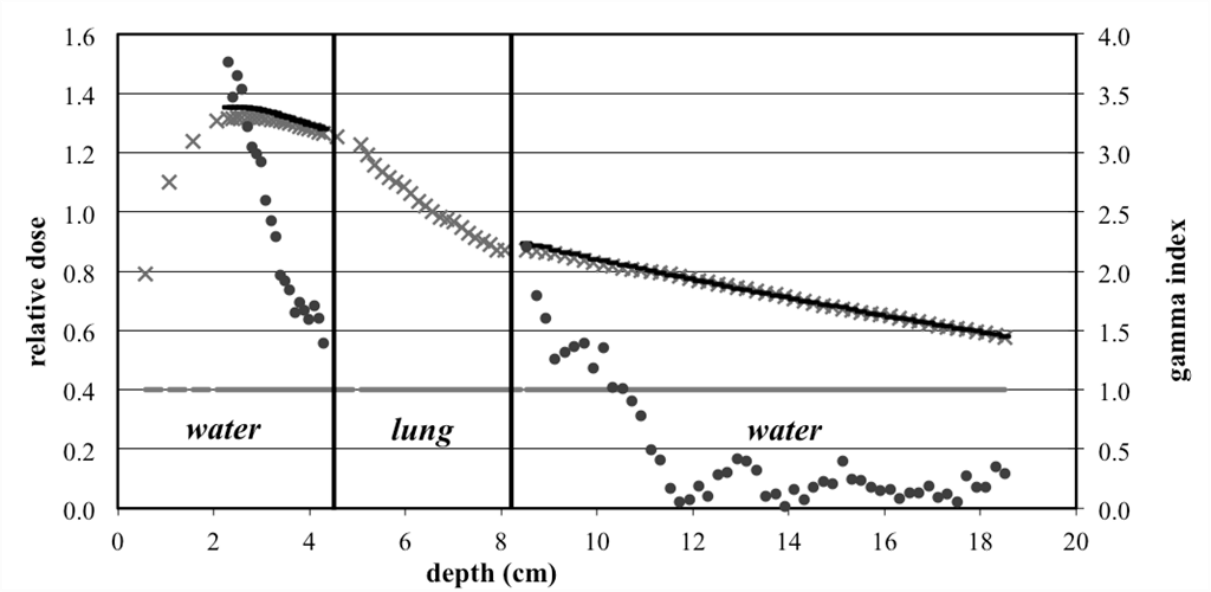

Figure 6. Depth dose curve (participants calculations (X) and measurements (-) data) and corresponding gamma index (**.**) (1%/1mm) for participant #1 (phantom A).

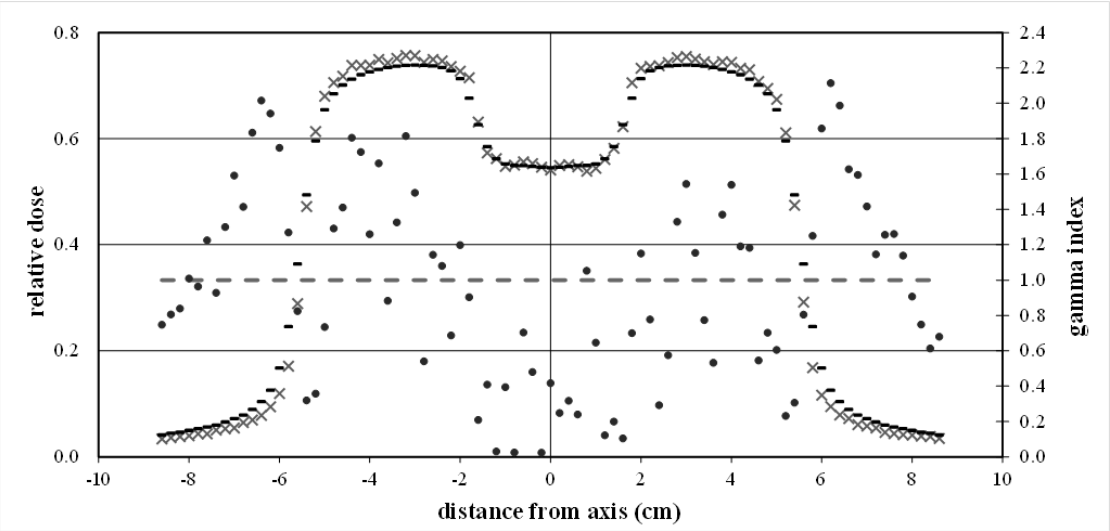

Figure 7. Dose profile (participants calculations (X) and measurements (-) data) and corresponding gamma index (**.**) (1%/1mm) for participant #3 (phantom D – 22 cm depth).